Available online at www.sciencedirect.com
SCIENCE DIRECT®
Journal of Magnetic Resonance 176 (2005) 71–78
JMR Journal of Magnetic Resonance
www.elsevier.com/locate/jmr

Spatially resolved emulsion droplet sizing using inverse Abel transforms

K.G. Hollingsworth, M.L. Johns *

Department of Chemical Engineering, University of Cambridge, Pembroke Street, Cambridge CB2 3RA, UK

Received 17 March 2005; revised 18 May 2005
Available online 22 June 2005

Abstract

Pulsed field gradient (PFG) nuclear magnetic resonance (NMR) is well established as a tool for determining emulsion droplet-size distributions via measurement of restricted self-diffusion. Most measurements made to date have not been spatially resolved, but have measured an average size distribution for a certain volume of emulsion. This paper demonstrates a rapid method of performing spatially resolved, restricted diffusion measurements, which enables emulsion droplet sizing to be spatially resolved as a function of radius in cylindrical geometries or pipes. This is achieved by the use of an Abel transform. The technique is demonstrated in various annular systems containing two emulsions, with different droplet-size distributions, and/or a pure fluid. It is also shown that by modifying the pulse sequence by the inclusion of flow-compensating magnetic field gradients, the technique can measure spatially resolved droplet-size distributions in flowing emulsions, with potential applications in spatially resolved on-line droplet-size analysis.

Keywords: Imaging; Abel transform; Emulsion; Restricted diffusion; Flow compensation

1. Introduction

The size distribution of emulsion droplets is an important measurement in liquid product design or formulation, as droplet size has an influence on the viscosity and stability of the emulsion, in addition to other product attributes. Pulsed field gradient (PFG) nuclear magnetic resonance (NMR) has been shown to be a useful tool for characterising the size distributions of a wide range of emulsions. Most work on emulsions to date measures the droplet-size distribution as a single distribution characteristic of the whole sample volume. However, it is not always the case that the emulsion sample will be spatially homogeneous. It has been shown that emulsion droplets can migrate under the influence of shear fields [1,2]. The spatial distribution of emulsion droplets is critical in certain process applications, e.g., suspension polymerisation [3]. It is therefore desirable to be able to measure emulsion droplet distributions with spatial resolution.

This can be achieved by using PFG NMR to create q-space encoding to measure the restricted diffusion of the ^{1}H of the discontinuous phase (usually oil) within emulsion droplets and to couple this with an appropriate imaging sequence. Such an approach was adopted by McDonald et al. [4], who recorded 1D vertical profiles of emulsion droplet size to measure the creaming behaviours of oil-in-water emulsions thickened with xanthan gum. From this, they assessed the role of depletion flocculation and stabilisation in the creaming process. Our work considers how to exploit the radial symmetry of a capillary or pipe (as encountered in most industrial process lines) to enable rapid imaging of the radial variation in emulsion droplet-size distribution. This approach is then extended to enable such spatially resolved measurements to be acquired on flowing streams.

* Corresponding author. Fax: +44 1223 334796.
E-mail address: mlj21@cam.ac.uk (M.L. Johns).

1090-7807/$ - see front matter © 2005 Elsevier Inc. All rights reserved.
doi:10.1016/j.jmr.2005.05.019

Nomenclature

a	Diameter of emulsion droplet	R	Signal attenuation due to diffusion in emulsion droplets
$b(g)$	Signal attenuation function	x	Profile coordinate
D	Self-diffusion coefficient, deformation of the droplet	α_m	Positive root of Eq. (2)
$F'(x)$	Derivative of intensity of profile	δ	Duration of pulsed field gradient
$F(r)$	Radial intensity function	ξ	Median of log-normal distribution
g	Gradient strength	Δ	Diffusion time
$P(a)$	Emulsion droplet-size distribution	γ	Gyromagnetic ratio
r	Radial distance	σ	Standard deviation of log-normal distribution

2. Theoretical development

In NMR, by applying a magnetic field gradient pulse to a sample, molecules are spatially encoded with a phase shift. A second magnetic field gradient pulse is applied at a later time, which reverses this phase shift. If none of the molecules have moved between the gradient pulses, the overall residual phase shift will be zero and the NMR signal will be completely refocused. Due to Brownian motion, however, the molecules will have moved between the gradient pulses, and the refocused signal will be attenuated. This signal attenuation is related to the self-diffusion coefficient, D, characterising Brownian motion by the well-known Stejskal–Tanner equation [5]. This technique is known as PFG NMR.

Within the discrete droplets of an oil-in-water emulsion, the oil molecules will undergo self-diffusion, but since the oil molecules cannot diffuse beyond the droplet surface, the molecules are only able to diffuse a fixed distance from their original positions. For a collection of molecules whose diffusion is restricted to within a spherical cavity, Murday and Cotts [6] calculated the following NMR signal attenuation expression:

$$\ln R(\Delta,\delta,a) = -2\gamma^2 g^2 \sum_{m=1}^{\infty} \frac{1}{\alpha_m^2(\alpha_m^2 a^2 - 2)} \times \left\{ \frac{2\delta}{\alpha_m^2 D} - \frac{2 + e^{-\alpha_m^2 D(\Delta-\delta)} - 2e^{-\alpha_m^2 D\Delta} - 2e^{-\alpha_m^2 D\delta} + e^{-\alpha_m^2 D(\Delta+\delta)}}{(\alpha_m^2 D)^2} \right\}, \tag{1}$$

where R is the signal attenuation, a is the droplet radius, D is the unrestricted self-diffusivity of the discrete phase liquid, and γ is the gyromagnetic ratio for the proton (2.675×10^8 rad/s T). δ is the duration of the pulsed field gradient, Δ is the diffusion or observation time, defined as the time between the leading edges of the two pulsed field gradients, and g is the magnitude of the pulsed field gradient. α_m is given by the positive roots of the following expression, where J_n is an nth order Bessel function:

$$J_{3/2}(\alpha a) = \alpha a J_{5/2}(\alpha a). \tag{2}$$

The model outlined by Eqs. (1) and (2) is known as the Gaussian phase distribution (GPD) model: it implicitly assumes that during the application of the pulsed field gradient the spins acquire a Gaussian distribution of phases—this is not verifiable experimentally but comparison with Monte Carlo simulations [7] of spins diffusing under these conditions shows the model to be accurate to at least 5% over the whole range of experimental conditions used in our work.

Packer and Rees [8] extended Eq. (1) to an emulsion with a probability distribution of radii, $P(a)$. Since the magnitude of the NMR signal received is proportional to the volume of material, a volume average of the attenuation function, $R(g,a)$ must be used

$$b(g) = \frac{\int_0^\infty a^3 P(a) R(g,a)\,da}{\int_0^\infty a^3 P(a)\,da}, \tag{3}$$

where $b(g)$ is the signal attenuation corresponding to a pulsed field gradient of magnitude g. Since $b(g)$ is not known as an analytical function, but rather as a discrete set of measurements contaminated by noise, it is not possible to directly extract $P(a)$ using Eq. (3). The probability distribution, $P(a)$, has usually been taken to be a log-normal distribution, given by:

$$P(a) = \frac{1}{2a\sigma(2\pi)^{1/2}} \exp\left\{ -\left[\frac{(\ln 2a - \ln \xi)^2}{2\sigma^2} \right] \right\}, \tag{4}$$

where σ is the shape parameter (variance) and ξ is the size parameter (median diameter). By imposing this two-parameter fit, the extraction of the droplet-size distribution is numerically stabilised.

The discrete phases of emulsion systems tend to have long T_1 relaxation times (~1 s) and short T_2 relaxation times (~10 ms). Since the magnetisation of the molecules in the droplets must be measured after several hundred milliseconds to observe restricted diffusion, it is necessary to base the acquisition pulse sequence on a stimulated echo. This is the approach adopted in the pulse sequence shown in Fig. 1, where a stimulated echo is acquired and the NMR PFG acquisition is combined with a 2D imaging sequence. Such a spatially resolved sequence is time consuming. By way of example, even using only eight different gradient values and a 64×64 image resolution with a phase cycle of 8 and a recycle time of 600 ms would give an experiment lasting 42 min. However, in many emulsion transport/processing scenarios we are interested in making droplet-size distribution measurements within pipes, which possess radial symmetry. It is possible to take advantage of this symmetry to reduce the acquisition time needed by using the discrete inverse Abel transform (DIAT), as was utilised in [9–12]. Using DIAT, it is possible to dispense with the phase gradient in the 2D imaging sequence and record only a 1D projection of the image intensity using a read gradient, which is then converted from cartesian into radial coordinates. For the example above, the acquisition time is reduced by a factor of 64. A similar result would be produced if an additional soft pulse and appropriate slice gradient were applied in Fig. 1 to select a slice across the diameter of the pipe. However, this would have an inherently poorer signal-to-noise and suffer from finite slice width effects in terms of defining the radial coordinate. Thus, we believe our approach, based on the application of DIAT, is both more accurate and more robust.

The inverse Abel transform enables a transformation from a 1D projection intensity measured in Cartesian coordinates, $F(x)$, to a radial intensity profile measured in radial coordinates from the centre of the object, $F(r)$. The relationship between $F(x)$ and $F(r)$ is given by [9]

$$F(r) = \int_r^\infty \frac{F'(x)\,\mathrm{d}x}{\sqrt{x^2 - r^2}}, \tag{5}$$

where $F'(x)$ is the first derivative of the projection intensity. Clearly, for practical purpose Eq. (5) must be discretized. A schematic of the projection data in Cartesian coordinates and its appearance after the inverse Abel transformation is given in Fig. 2 for a homogeneous pipe. It is also possible to produce a flow-compensated version of the pulse sequence in Fig. 1, by the use of a double stimulate echo and the addition of an additional pair of pulsed field gradients before the imaging part of the sequence, as shown in Fig. 3. Such flow compensation was demonstrated previously for spatially unresolved measurements of emulsion droplet size [13]. Thus, we are able to measure the radial variation in emulsion droplet-size distributions in a pipe for a flowing stream.

When combining NMR PFG with imaging (as in the pulse sequences shown in Figs. 1 and 3), there is no spectroscopic resolution, unlike in the non-spatially resolved diffusion measurements of emulsion droplet-size distribution, where the full spectrum is available for use. To be sure that we measure the restricted diffusion from the discrete droplet phase only, the same principle is used as when measuring diffusion (to size emulsion) with a magnetic field too small to give spectral discrimination [14]: the water in the continuous phase is much more mobile so that the signal effectively disappears under the influence of the diffusion gradients and consequently only the oil signal remains. If this were not true (if the continuous fluid were a long-chain polymer, for example, with a very low diffusion coefficient) then we could discriminate on the basis of T_1 relaxation times by using a 180° inversion recovery pulse prior to each scan of the sequence (for such an application of inversion recovery to the selective detection of diffusion within emulsion droplets, see [15]) or use a chemically selective pulse to

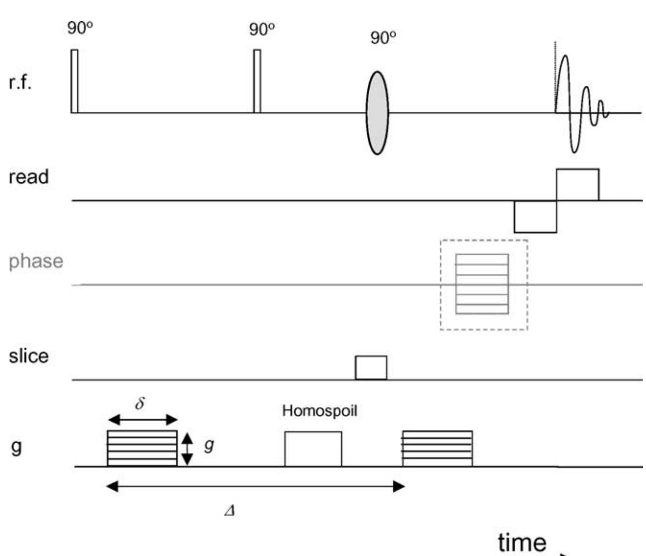

Fig. 1. Stimulated echo 2D imaging sequence for diffusion measurement. The dotted box indicates the phase gradient removed to produce fast 1D profiles for processing with DIAT to render radial distributions.

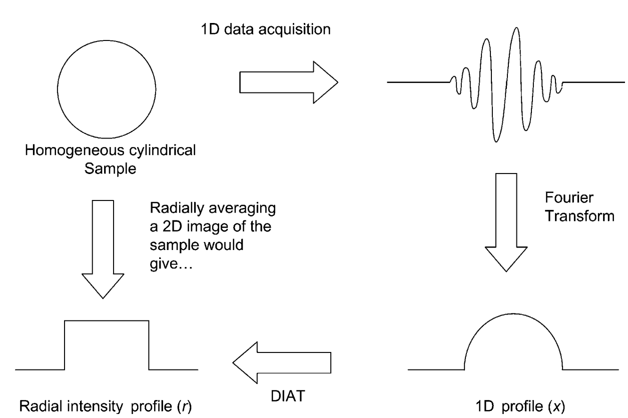

Fig. 2. Schematic of the relationship between the 1D raw time-domain data acquired, the Cartesian data after Fourier transformation, and the radial data post-DIAT (note this corresponds to a radial average of a 2D image of the sample).

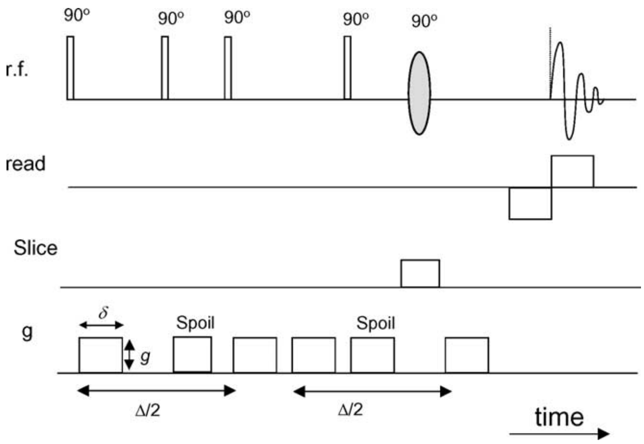

Fig. 3. Pulse sequence, with flow compensation, to produce profiles for inverse Abel transformation of flowing materials to render diffusion information.

select the oil phase (as demonstrated for a velocity measurement in [16]).

3. Experimental

To demonstrate application of the discrete inverse Abel transform (DIAT) method, several annular liquid/emulsion systems were constructed to test the integration of the PFG NMR measurement into the 1D imaging pulse sequence (Fig. 1), the data being subsequently subjected to DIAT followed by emulsion droplet sizing where appropriate. The inclusion of flow compensation into this pulse sequence was then tested using water, followed by an oil-in-water emulsion, flowing in a pipe. Results were compared with suitable stationary measurements.

3.1. Measurement within an annular system

We wished to produce an experimental geometry with cylindrical symmetry that had two separate annular compartments. Emulsions with different droplet-size distributions could then be introduced into the two compartments and we could compare the spatially resolved droplet-size distributions (as a function of radius) with those recorded without spatial resolution. A 5 mm outer diameter NMR tube was placed inside a 9.6 mm inner diameter NMR tube to form two such annular compartments and two different experiments were considered: Experiment A used 5 cS dimethylpolysiloxane (silicone oil) in the inner compartment and a silicone oil-in-water emulsion (20 wt% Tween 20 as the surfactant) in the outer compartment. Experiment B used a silicone oil-in-water emulsion (5 wt% Tween 20 as the surfactant) in the inner compartment and a silicone oil-in-water emulsion (1 wt% Tween 60 as the surfactant) in the outer compartment. All chemicals were purchased from Sigma–Aldrich, UK. Further experimental details are listed in Table 1.

3.2. Flow-compensated measurements of flow in a pipe

Distilled water was convected through a glass pipe (inner diameter of 10.8 mm) at a flowrate of 80 ml/min (corresponding to an average velocity of 14.5 mm/s, which corresponded to laminar flow). Diffusion measurements were acquired using the flow-compensated pulse sequence shown in Fig. 3 and subsequently subjected to DIAT followed by determination of the spatially resolved diffusion coefficients. A stationary measurement was also taken for comparison. The experimental conditions used were: $\delta = 1$ ms, $\Delta = 50$ ms, and the gradient field strength (g) was varied from 2 to 40 G/cm in 16 steps.

A toluene-in-water emulsion was produced by dissolving 1.5 vol% Triton X-100 (non-ionic surfactant, purchased from Sigma–Aldrich, UK) in distilled water and then dispersing toluene (purchased from Sigma–Aldrich, UK) in the water-surfactant solution using a high shear mixer. Equal volumes of toluene and water were used (48.5 vol%). Spatially resolved emulsion droplet-size distributions were measured under both stationary conditions and under steady flow within a closed flow loop driven by gravity. The flowrate used was 25 ml/min. This corresponds to a superficial velocity of 4.55 mm/s, the emulsion density was estimated to be 0.932 kg/m^3; the viscosity of the emulsion has been measured on a parallel plate viscometer to be 10 mPa, and the inner diameter of the tube used is 10.8 mm: therefore, the Reynolds number for this flow is 5 (laminar flow). The emulsion was not found to be significantly shear-thinning at this concentration. The experimental conditions used were: $\delta = 5$ ms,

Table 1
Details of emulsion systems and experimental parameters used with the annular geometry

System	Fluid in inner tube	Fluid in annulus	PFG duration δ (ms)	Observation time Δ (ms)	PFG magnitude (G/cm)
A	5 cS silicone oil (pure fluid)	Silicone oil-in-water emulsion (20% Tween 20)	5	500	2–80 in 16 steps
B	Silicone oil-in-water emulsion (5% Tween 20)	Silicone oil-in-water emulsion (1% Tween 60)	5	500	2–80 in 16 steps

$\Delta = 100$ ms, and the gradient field strength (g) was varied from 2 to 80 G/cm in 16 steps.

3.3. Data analysis

In the case of emulsion systems, once the DIAT algorithm (Eq. (5)) had been applied to the data, the attenuation curves for each pixel in the radial profile were then processed to produce an emulsion droplet-size distribution. Droplet-size distributions were extracted by application of Eqs. (1)–(4); further details of the models and the fitting process can be found in [17].

4. Results and discussion

4.1. Measurement within an annular system

For Experiment A, the 3D mesh plot of the Fourier transformed signal intensity data is given in Fig. 4A (in Cartesian coordinate) against position, x, across the pipe and gradient strength, g. The corresponding data, as is produced by the DIAT algorithm, are shown in Fig. 4B where radial position, r, has replaced position across the pipe. It is clearly seen that the signal from the pure silicone oil in the inner compartment of the tube decays much more rapidly than the silicone oil in the emulsion, which is subject to restricted diffusion. (For the pure oil, there are only four points before the signal descends into the noise level, compared to the silicone oil in the emulsion, which gives a signal at all gradient values due to its diffusion being restricted). Using the Stejskal–Tanner equation to fit the points for the pure silicone oil in the inner compartment, the measured diffusion coefficient is 1.18×10^{-10} m^2/s (the variation with radius is not systematic and results in a standard deviation of only 0.1×10^{-10} m^2/s). This is in good agreement with the value of D for silicone oil measured with conventional NMR PFG techniques: 1.20×10^{-10} m^2/s. Application of Eqs. (1)–(4) to the data for the silicone oil-in-water emulsion in the outer annulus or compartment produces a log-normal curve of $\sigma = 0.912$ (standard deviation is 0.12) and $\xi = 1.9$ μm (standard deviation is 0.3 μm) (refer to Eq. (4)) for the emulsion droplet-size distributions. The standard deviations arise from the variation across the profile with radius; this variation is not systematic indicating that the methodology is working. An unresolved measurement of the emulsion droplet-size distribution yields: $\sigma = 0.86$ and $\xi = 2.1$ μm, which is in good agreement with the spatially resolved measurements.

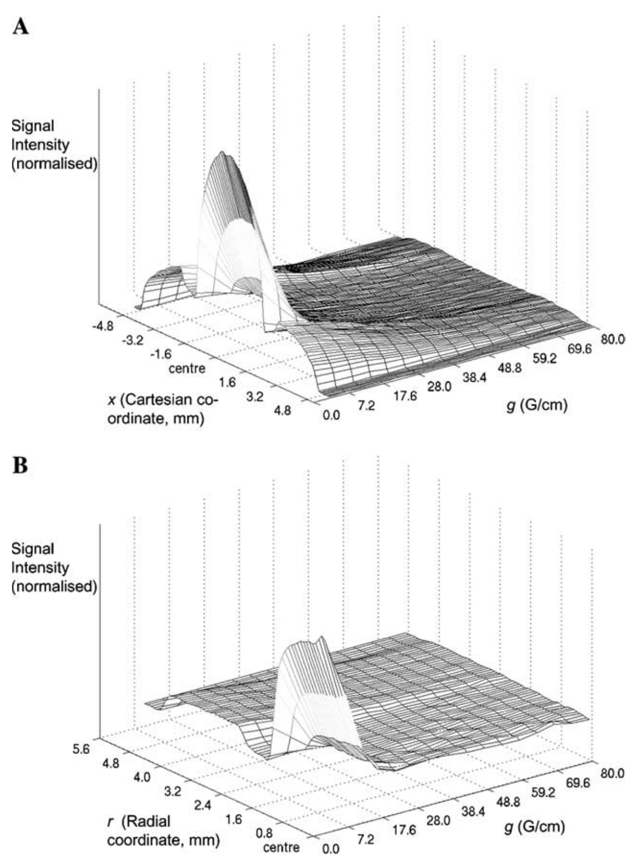

Fig. 4. (A) Fourier transformed data and (B) attenuation (signal intensity) data plotted against gradient strength and radial position for pure substance/emulsion annular system (Experiment A).

For Experiment B (two different emulsions), the attenuation data (signal intensity) following Fourier transformation and processing with the DIAT algorithm are presented in Fig. 5A. The attenuations for the two emulsions are quite noticeably different. In Fig. 5B, the average emulsion droplet-size distributions for the emulsion in the inner compartment (inner emulsion) and the emulsion in the outer annulus (emulsion in annulus) are shown. Clearly, the inner emulsion features significantly smaller emulsion droplets than the emulsion in the outer annulus. This is what is expected given the larger surfactant content of the inner emulsion (as detailed in Table 1) and the identical mixing regime to which the emulsions were subjected. Unresolved measurements for the two emulsions, measured individually using conventional NMR PFG, are also shown in Fig. 5B and clearly are in excellent agreement with the spatially resolved measurements. Within each emulsion system there was no systematic variation in the emulsion size distribution measured with radial position: this is as expected and shows that the technique can measure emulsion droplet-size distributions reliably.

4.2. Flow-compensated measurement of the self-diffusion coefficient of water

In the case of a pure fluid, such as water, Taylor dispersion occurs where molecules diffuse across flow streamlines [18]. This causes them to change velocity

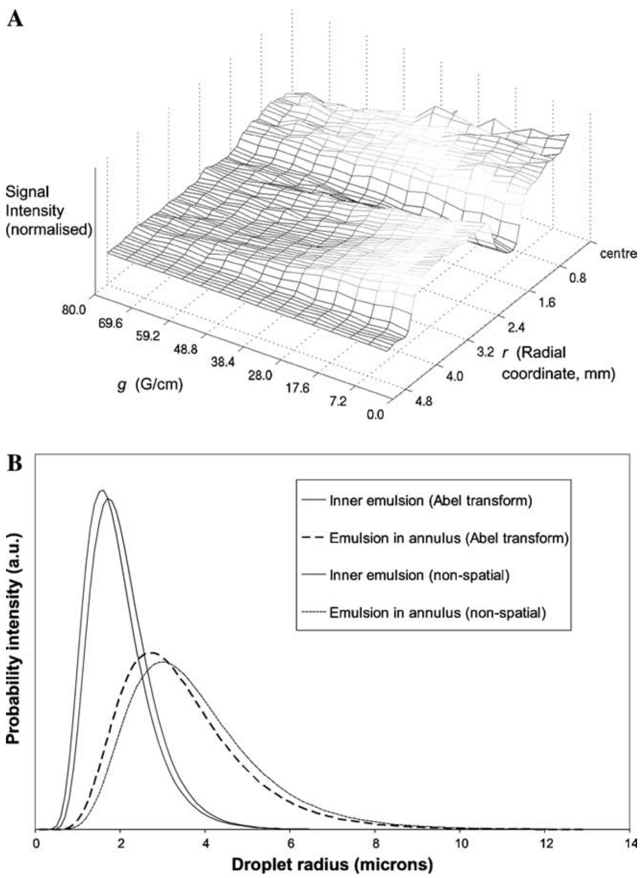

Fig. 5. (A) Attenuation data plotted against gradient strength and radial position for the annular system with two different emulsions. (B) Comparison of droplet-size distributions for inner emulsion and emulsion in annulus, derived from both Abel transform and non-spatially resolved measurements.

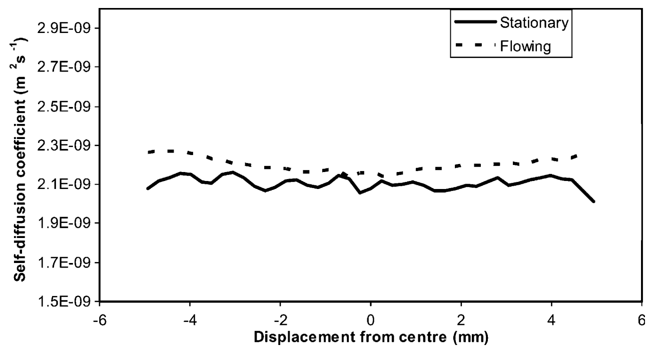

Fig. 6. Radial map of the self-diffusion coefficients of distilled water measured for stationary and laminar flowing (80 ml/min, Reynolds number = 167) conditions using the pulse sequence in Fig. 3 and the DIAT algorithm. The data were analysed in two halves about the centre of the tube.

during the diffusion measurement time, Δ, and hence the flow compensation (as employed in the pulse sequence shown in Fig. 3) will either under- or over-compensate flow effects leading to further attenuation of the signal. This manifests itself as additional attenuation or equivalently as an increase in the apparent diffusion coefficient.

The self-diffusion coefficient was calculated for each radial position in the pipe following application of DIAT to the profile intensity data, and the results are presented in Fig. 6 for both stationary and flowing water. The average value for stationary water of 2.1×10^{-9} m^2/s is what is expected at a room temperature of 20 °C; there is also no systematic variation with radius, as expected. For the flowing water, the enhancement of the self-diffusion coefficient for the flowing water is ~3% in the centre of the pipe and ~8% at the edge of the pipe. This is a consequence of Taylor dispersion; the greater enhancement with radial position away from the pipe centre results from the increased velocity shear experienced with increased radius away from the centre of the pipe in laminar flow. If there is significant shear across a pixel, the increased spread of velocities increases the effect of Taylor dispersion within a pixel, which enhances the apparent self-diffusion coefficient. Thus, we are measuring the expected behaviour which gives us confidence in the inclusion of the DIAT algorithm into the flow-compensated spatially resolved emulsion droplet-sizing technique.

4.3. Flow-compensated measurement of a toluene-in-water emulsion

The droplet-size distribution as a function of radius for the stationary toluene-in-water emulsion is presented in Fig. 7A, the corresponding result for the flowing emulsion is shown in Fig. 7B. The droplet-size distributions are very similar for both systems—the average parameters characterising the droplet-size distribution for the stationary emulsion are: $\sigma = 0.406$ (standard deviation of 0.005), $\xi = 3.3$ μm (standard deviation of 0.16 μm), the corresponding data for the flowing emulsion are: $\sigma = 0.416$ (standard deviation of 0.028), $\xi = 3.4$ μm (standard deviation of 0.22 μm). The maximum capillary number experienced by the emulsion droplets in these flowing experiments is $\sim 1 \times 10^{-4}$ and hence there is minimal possibility of droplet break-up in the laminar flow (which would require a capillary number of order unity [19]) of the emulsion system considered. The agreement between Figs. 7A and B shows that the flow compensation is successful.

No radial variation occurs in the emulsion droplet-size distribution observed for either sample. In the case of the stationary emulsion (Fig. 7A) this is entirely expected, in the case of the flowing emulsion (Fig. 7B), this indicates that there has been no significant migration of droplets across the tube. Emulsion droplets under shear flow will tend to migrate away from the bounding walls due to asymmetry in the flow around the deformed droplet: the rate of migration depends on factors such as the size of the droplets (larger drop-

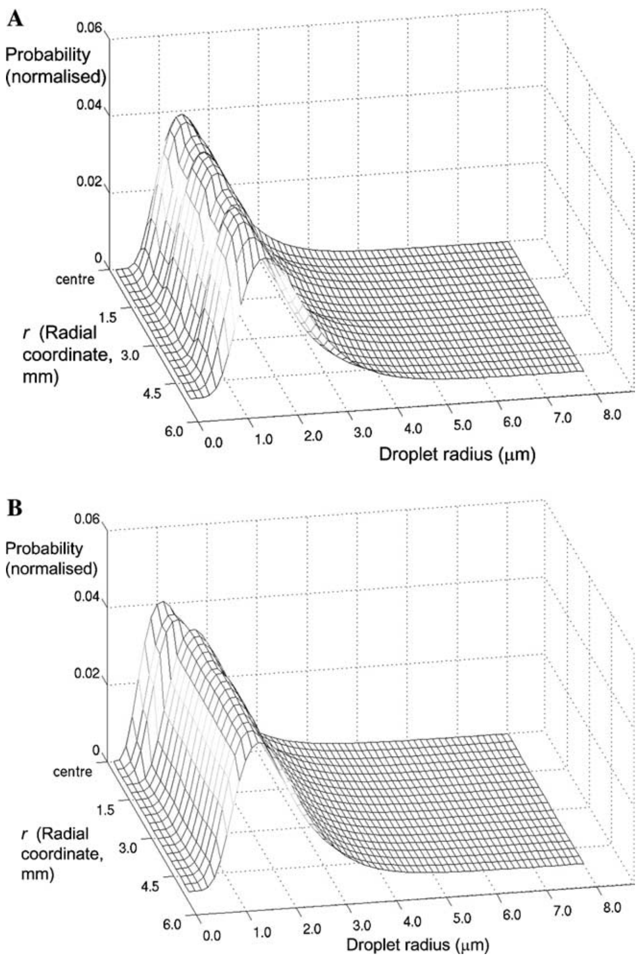

Fig. 7. Droplet-size distributions plotted against radial dimension for (A) stationary toluene-in-water emulsion and (B) flowing toluene-in-water emulsion.

lets will migrate faster) and the viscosity of the continuous phase [20]. According to the theory presented in [20], a droplet of diameter 10 μm (the largest droplet size observed in the stationary emulsion) with the system considered here will migrate 5×10^{-9} m (0.005 μm) over the 30 cm that the flow is developed. This is several orders of magnitude smaller than the droplet size itself and hence insignificant droplet migration is to be expected, as is observed in Fig. 7B. The Taylor dispersion effect, observed in Fig. 6 for free water, will be negligible for emulsion droplets, as the self-diffusivity of emulsion droplets which have radii of several microns will be several orders of magnitude lower than that of pure water.

5. Conclusion

This study shows that the discrete inverse Abel transform (DIAT) is a suitable method of measuring spatially resolved emulsion droplet sizes in a time-saving manner for a classic and typical geometry, that being a pipe. The cylindrical geometry is common in industrially important process applications (such as petrochemicals, pharmaceuticals, foodstuffs, and consumer goods) where emulsions may be present as products or intermediates. Furthermore, it has been shown that the technique can be applied to emulsions that are undergoing laminar flow, and to consequentially measure radial variations in droplet size for flowing emulsions. Future work will apply this technology to on-line analysis of the output from experimental industrial emulsification devices.

Acknowledgments

The EPSRC are thanked for the provision of a Quota Studentship award for Kieren Hollingsworth. The assistance of Mick Mantle, Andrew Sederman, and Melanie Britton with respect to NMR pulse sequence development is acknowledged.

References

[1] M.R. King, D.T. Leighton, Measurement of shear-induced dispersion in a dilute emulsion, Phys. Fluids 13 (2) (2001) 397–406.
[2] H.L. Goldsmith, S.G. Mason, The flow of suspensions through tubes: I. Single spheres, rods and discs, J. Colloid Sci. 17 (1962) 448–476.
[3] P.J. Dowding, B. Vincent, Suspension polymerisation to form polymer beads, Colloids Surf. A 161 (2000) 259–269.
[4] P.J. McDonald, E. Ciampi, J.L. Keddie, M. Heidenreich, R. Kimmich, Magnetic resonance determination of the spatial dependence of the droplet-size distribution in the cream layer of oil-in-water emulsions: evidence for the effects of depletion flocculation, Phys. Rev. E 59 (1999) 874–884.
[5] E.O. Stejskal, J.E. Tanner, Spin diffusion measurements: spin echoes in the presence of a tine-dependent field gradient, J. Chem. Phys. 42 (1965) 288–292.
[6] J.S. Murday, J.M. Cotts, Self-diffusion coefficient of liquid lithium, J. Chem. Phys. 48 (1968) 4938.
[7] B. Balinov, B. Jonsson, P. Linse, O. Soderman, The NMR self-diffusion method applied to restricted diffusion. Simulation of echo attenuation from molecules in spheres and between planes, J. Magn. Reson. A 104 (1993) 17.
[8] K.J. Packer, C.J. Rees, Pulsed NMR studies of restricted diffusion: I. Measurement of emulsion droplet sizes, J. Colloid Interface Sci. 10 (1971) 206–208.
[9] P.D. Majors, A. Caprihan, Fast radial imaging of circular and spherical objects by NMR, J. Magn. Reson. 94 (1991) 225–233.
[10] S.J. Gibbs, D.E. Haycock, W.J. Frith, S. Ablett, L.D. Hall, Strategies for rapid NMR rheometry by magnetic resonance imaging velocimetry, J. Magn. Reson. 125 (1997) 43–51.
[11] B.P. Hills, J. Godward, K.M. Wright, Fast radial NMR microimaging studies of pasta drying, J. Food Eng. 33 (1997) 321–335.
[12] S.G. Harding, H. Baumann, Nuclear magnetic resonance studies of solvent flow through chromatographic columns: effect of packing density on flow patterns, J. Chromatogr. A 905 (2001) 19–34.
[13] M.L. Johns, L.F. Gladden, Sizing of emulsion droplets under flow using flow-compensating NMR-PFG techniques, J. Magn. Reson. 154 (2002) 142–145.

[14] G.J.W. Goudappel, J.P.M. van Duynhoven, M.M.W. Mooren, Measurement of oil droplet size distributions in food oil/water emulsions by time domain pulsed field gradient NMR, J. Colloid Interface Sci. 239 (2001) 535–542.
[15] J.P.M. van Duynhoven, G.J.W. Goudappel, G. van Dalen, P.C. van Bruggen, J.C.G. Blonk, A.P.A.M. Eijkelenboom, Scope of droplet size measurements in food emulsions by pulsed field gradient NMR at low field, Magn. Reson. Chem. 40 (2002) S51–S59.
[16] B. Newling, S.J. Gibbs, L.D. Hall, D.E. Haycock, W.J. Frith, S. Ablett, Chemically resolved NMR velocimetry, Chem. Eng. Sci. 52 (1997) 2059–2072.
[17] K.G. Hollingsworth, M.L. Johns, Measurement of emulsion droplet sizes using PFG NMR and regularization methods, J. Colloid Interface Sci. 258 (2003) 383–389.
[18] S.L. Codd, B. Manz, J.D. Seymour, P.T. Callaghan, Taylor dispersion and molecular displacements in Poiseuille flow, Phys. Rev. E 60 (1999) R3491–R3494.
[19] H.P. Grace, Dispersion phenomena in high viscosity immiscible fluid systems and application of static mixers as dispersion devices in such systems, Chem. Eng. Commun. 14 (1982) 225–277.
[20] P.C.H. Chan, L.G. Leal, The motion of a deformable drop in a second-order fluid, J. Fluid Mech. 92 (1979) 131–170.